Blackbody Infrared Radiative Dissociation of Partially Solvated Mixed Ligand Ru(II) Complex Ions†

Stanley M. Stevens, Jr.,[¶,#] Robert C. Dunbar,[+] William D. Price,[@] Marcelo Sena,[£] Clifford H. Watson,[¶,§] Linda S. Nichols,[¶,‡] Jose M. Riveros,[£] David E. Richardson,[¶] and John R. Eyler*

Department of Chemistry, P. O. Box 117200, University of Florida, Gainesville, Florida 32611-7200, Chemistry Department, Case Western Reserve University, Cleveland, Ohio 44106, Department of Chemistry, Marshall University, Huntington, West Virginia 25755, and Universidade de São Paulo, Instituto de Química, São Paulo -SP- Brazil, Caixa Postal 26077, CEP 05599-970

Received: April 8, 2004; In Final Form: June 29, 2004

Unimolecular dissociation reactions of gas-phase partially solvated transition metal complex ions, diamminebis-(2,2′-bipyridine)ruthenium(II), $[Ru(NH_3)_2(bipy)_2]^{2+}$, tetraammine(2,2′-bipyridine)ruthenium(II), $[Ru(NH_3)_4$-$bipy]^{2+}$, and pentaammine(2-methylpyrazine)ruthenium(II), $[Ru(NH_3)_5MePyz]^{3+}$, have been investigated with electrospray ionization Fourier transform ion cyclotron resonance mass spectrometry (ESI−FTICR/MS) under low pressure ($<10^{-8}$ mbar) conditions. Under these conditions, dissociation of solvent from the complex ions is driven primarily by absorption of blackbody photons from the FTICR analyzer cell walls, that is, via blackbody infrared radiative dissociation (BIRD), with little collisional contribution at pressures below 10^{-8} mbar. The replacement of ammine hydrogens with deuterium increases measured BIRD rate constants. Optimized geometries, vibrational frequencies, and IR absorption band intensities have been calculated for the complexes by semiempirical and ab initio methods. These calculated parameters have been employed in master equation modeling of the desolvation reactions to extract dissociation energetics. Solvation energies obtained by master equation modeling were found to be in the range 19 ± 1 kcal/mol for the dissociation of acetone from various mixed ligand Ru(II) complex ions studied in this work. This is about 4 kcal/mol higher than for the comparable complexes containing only bipyridyl ligands and no ammine ligands.

Introduction

Useful insights into the similarities and differences between solution and gas-phase chemistry can come from the study of partially solvated gas phase ions, providing a bridge between the properties of the completely unsolvated gas phase ions and the same fully solvated species in solution. Contemporary experimental approaches can characterize the processes involved in this progressive solvation of gas-phase ions, and in particular can measure the energies of stepwise attachment of individual solvent molecules. Especially interesting for such stepwise solvation studies are coordination complexes containing ruthenium and bipyridyl ligands, whose properties and excited-state chemistry and photochemistry have been subjects of widespread investigation. In particular, polypyridine complexes of divalent ruthenium ions have been of major interest for applications such as analytical chemiluminescence[1] and solar energy conversion.[2] A variety of chemical and physical techniques have been applied to study these compounds,[3,4] among which the relatively new approach of blackbody infrared radiative dissociation (BIRD)[5−7] is the particular focus of the work described here.

The use of BIRD to characterize gas-phase unimolecular dissociation reactions of trapped ions, both kinetically and energetically, has been quite successful in recent years.[8−36] Results in a previous paper[37] (hereafter referred to as Paper I) showed that analysis assuming a BIRD mechanism allowed determination of the zero-pressure activation energies of gas-phase desolvation reactions for a variety of solvent molecules attached to transition metal complex ions. Using careful modeling of kinetics and determination of vibrational properties, binding energies indicative of the true solvate dissociation energy can be obtained. Consequently, BIRD analyses to determine solvation energetics can be a powerful tool to explore the role of solvent on structure and reactivity. For example, work by Williams et al.[29] has shown that small DNA molecules retain Watson−Crick base pairing in the gas-phase, a property critical for solution-phase DNA structure. Additionally, the same group has examined a variety of metal ion/arginine complexes and commented on the factors that lead to a gas-phase zwitterionic structure.[30]

Dissociation processes can be observed at low pressures by Fourier transform ion cyclotron resonance mass spectrometry (FTICR/MS). When the observed kinetics are found to be incompatible with the Lindemann-Christiansen model for dissociation, which is based on collisional energy-exchange processes, this is taken as evidence for the BIRD mechanism. One of the main advantages of the BIRD technique is that ions

† Part of the special issue "Tomas Baer Festschrift".

* Corresponding Author E-mail Address: eyler@chem.ufl.edu.
¶ University of Florida.
+ Case Western Reserve University.
@ Marshall University.
£ Universidade de São Paulo.
Current Address: Protein Chemistry Core, Interdisciplinary Center for Biotechnology Research, University of Florida, Gainesville, Florida 32610-0156.
§ Current Address: Centers for Disease Control and Prevention, Air Toxicants Branch, Atlanta, Georgia 30341-3724.
‡ Current Address: Savannah River Technology Center, Westinghouse Savannah River Company, Aiken, South Carolina 29808.

10.1021/jp0484377 CCC: $27.50
Published on Web 08/10/2004

can be modeled with well-characterized internal energy distributions, which can be described by Boltzmann (or modified Boltzmann) statistics.[18] This makes BIRD an effective tool for determining dissociation thermochemistry of gas-phase complexes, including the determination of binding energies of solvent molecules to partially solvated molecules.

In the present study, unimolecular dissociation reactions of gas-phase partially solvated mixed ligand ruthenium(II) complex ions have been studied to probe effects of variation in complex ion ligation upon solvation around the metal complex ion. This approach offers insight into the fundamental aspects of the impact of solvation on ion structure, reactivity, and energetics. In Paper I, solvation thermochemistry was investigated for Ru(II) complexes whose inner shell of ligands consisted entirely of bipyridyl (bipy) ligands. The present report extends this work to complexes whose inner complexation shell contains NH_3 ligands as well as bipy ligands. In addition to experimental results, various theoretical methods have been used to explore the energetics of first solvation shell interactions.

Experimental Section

All experiments were performed with a Bruker BioAPEX 4.7 T FTICR mass spectrometer (Bruker Analytical Systems, Billerica, MA) coupled to a modified external Analytica (Branford, CT) electrospray ionization source (ESI) described in detail in Paper I.[37] Sample introduction into the ESI source was performed using a 250-μL syringe at a flow rate of 60 μL/hr. An N_2/solvent gaseous mixture was introduced into the ESI source housing to generate the partially solvated metal complex ions used in the subsequent kinetic study by BIRD. This resolvation technique[38] is advantageous in that cluster formation is independent of the ESI process and clusters form by association of solvent molecules with ionic species after they have been transferred from solution to gas phase. Critical factors influencing the resolvation process are the capillary temperature, the flow rate of the solvent-carrier gas into the ESI source housing, and the diameter of the exit orifice of the heated capillary.

The source region pressure was maintained by an Edwards 800 L/s cryo pump with subsequent pumping supplied by two Edwards 400 L/s cryo pumps. This particular pump arrangement provides sufficient differential pumping to obtain low base pressures (10^{-9} mbar) in the FTICR analyzer cell even when coupled to an atmospheric pressure ionization technique. The capillary temperature was maintained at 100−110 °C. Ions exiting the ESI source were collected in a hexapole ion trap/guide for a period of 1 s before being transferred to the FTICR mass analyzer cell. Ions were mass selected in the FTICR cell with a standard correlated frequency sweep[39] corresponding to the mass range of interest. Ion peak heights were monitored at various reaction delay times to determine dissociation rate constants.

Pressure dependence studies were performed by introducing argon directly into the FTICR cell via Varian leak valves (Lexington, MA, Model 951-5106) located near the analyzer cell region. Our earlier work described in Paper I[37] showed that BIRD rates for ruthenium complex ion/solvent bond dissociation were essentially pressure independent within the pressure range 10^{-8}−10^{-9} mbar. Temperature dependence studies were performed by heating the vacuum chamber around the ICR analyzer cell and measuring the temperature of two copper−constantan thermocouples placed in the electrically insulated structures that support the two opposing trapping electrodes, with the average of the two taken as the temperature in the cell. Calibration was accomplished with a third thermocouple placed directly in the center of the cell (only during calibration experiments). The average temperature from the two thermocouples at either end of the cell was always found to be within ±3 K of the third thermocouple reading over a temperature range of 294−365 K.

Deuterium exchange with hydrogen was accomplished using deuterated methanol as a solvent for $[Ru(NH_3)_5MePyz]^{3+}$. Since deuterated alcohols are known to undergo solution-phase H/D exchange reactions with the ammine group hydrogens, the ion peaks in the mass spectrum corresponding to a five unit increase in mass-to-charge ratio were assigned as $[Ru(ND_3)_5MePyz]^{3+}$-$(solvent)_n$ and isolated for subsequent BIRD kinetic studies.

Computational Section

Theoretical Calculations. Geometries of partially solvated Ru(II) complex ions were calculated using ZINDO[40,41] semiempirical methods. Vibrational frequencies and IR absorption intensities were calculated using the same computational method, and employed for subsequent master equation analysis. As described in Paper I,[37] the ZINDO frequencies were scaled according to an empirical scaling equation. The vibrational frequencies from ZINDO are in reasonable agreement with ab initio and experimental values.

Calculations of various properties of $[Ru(NH_3)_6]^{2+}(acetone)_1$, $[Ru(NH_3)_4(bipy)]^{2+}(acetone)_1$, $[Ru(NH_3)_4(bipy)]^{2+}(acetonitrile)_1$, $Ru(NH_3)_2(bipy)_2^{2+}$, and $Ru(bipy)_3^{2+}$ were also performed using the Gaussian 98[42] computational package. The geometry of each species was first optimized using ZINDO and then used as the input for density functional theory (DFT) calculations at the B3LYP/LANL2DZ level of theory. These DFT calculations provided the final optimized structures, as well as the vibrational frequencies and absolute absorption intensities. The LANL2DZ basis set uses an effective core potential developed by Hay and Wadt[43−45] (Los Alamos National Laboratories) plus the DZ basis set to describe the elements Na to Bi. The Dunning/Huzinaga full double-ζ (D95)[46] basis set was used for the first row elements.

Kinetic Modeling. The dissociation kinetics for desolvation of the partially solvated ruthenium clusters were modeled using the same master equation approaches that were described in detail in Paper I,[15,20,37,47] and only a brief summary will be given here. Two master equation modeling programs, similar in concept but differing in some computational details, were used: one at Marshall University and one at Case Western Reserve University. Briefly, the master equation model numerically simulates the experiment as the solution to a set of coupled differential equations explicitly accounting for the detailed rates of all state-to-state transitions and dissociation processes. The microcanonical dissociation rates were determined either from RRKM theory or Phase Space Theory using the reactant and transition state frequency sets described above. As noted above, an empirical scaling formula was applied to the transition frequencies calculated at the ZINDO semiempirical level; DFT frequencies were scaled by 0.94.

Within the master equation model variation of three parameter types can be made to fit the experimental Arrhenius constants: the threshold dissociation energy (E_0), the oscillator transition dipole moments (μ), and the transition frequency set associated with the activation entropy ($\Delta S^{\dagger}$).The master equation modeled threshold dissociation energies were obtained in the Marshall University treatment by systematically varying and optimizing all three of these parameters by comparison of the resulting activation parameters with the experimental values. Typically, only a narrow range of E_o values were consistent with fitting within the allowed tolerances.

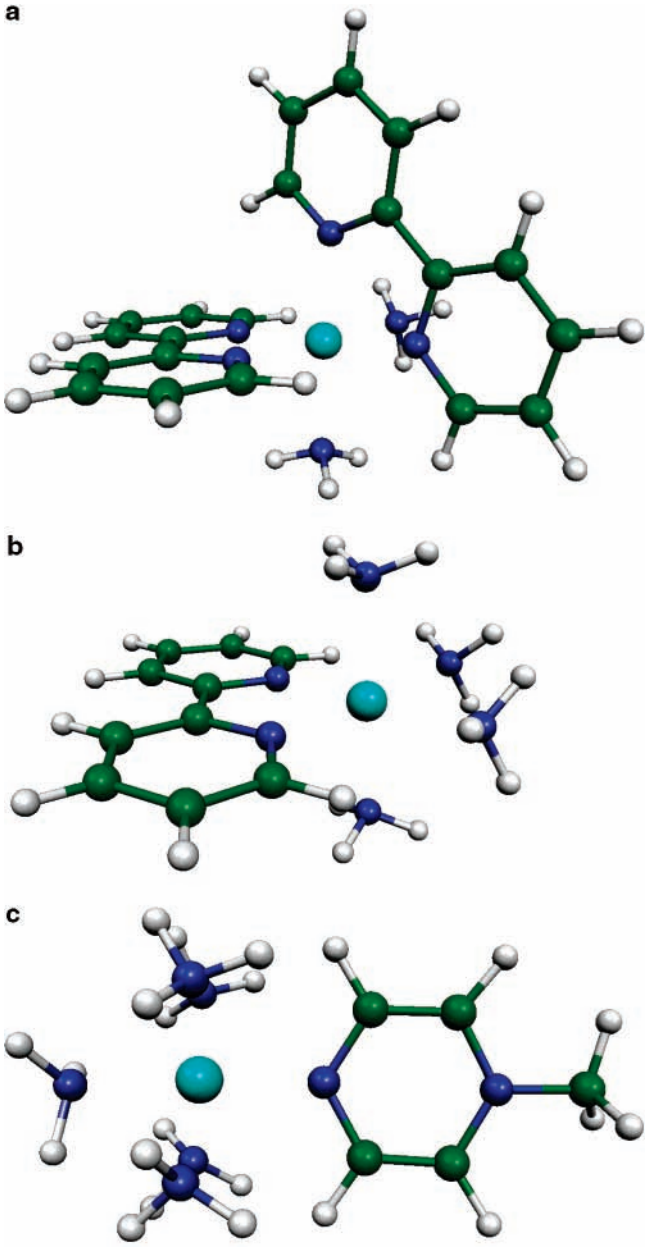

Figure 1. Cartoon structures of (a) $[Ru(NH_3)_2(bipy)_2]^{2+}$, (b) $[Ru(NH_3)_4(bipy)]^{2+}$, and (c) $[Ru(NH_3)_5(MePyz)]^{3+}$. The nitrogens of the ammine, methylpyrazine, and bipyridine ligands are coordinatively bound to the central ruthenium ion to form an octahedral-like complex.

In the Case Western Reserve University treatment, the calculated transition dipole moments were used without adjustment, and only two parameters, E_o and $\Delta S\ddagger$, were considered as adjustable in the RRKM-based fits. A substantial range of values of these parameters gave believable fits to the experimental results. As in Paper I,[37] this range of possibilities was narrowed by assuming a reasonably loose transition state ($\Delta S\ddagger$ of 10 cal K^{-1} mol^{-1}) in the RRKM dissociation modeling. In addition, a set of fits was generated using phase-space theory (PST) dissociation modeling, representing the extreme limit of a loose transition state. PST modeling has generally been considered to reflect an unreasonably loose transition state for most systems, and the fitting results given here from this approach are included to suggest the degree of uncertainty in the modeling procedure resulting from the lack of knowledge about the appropriate transition state for this aspect of the kinetic modeling. Paper I[37] gives an extended discussion of the assumptions and limitations of models used for the transition state in these solvent dissociation processes.

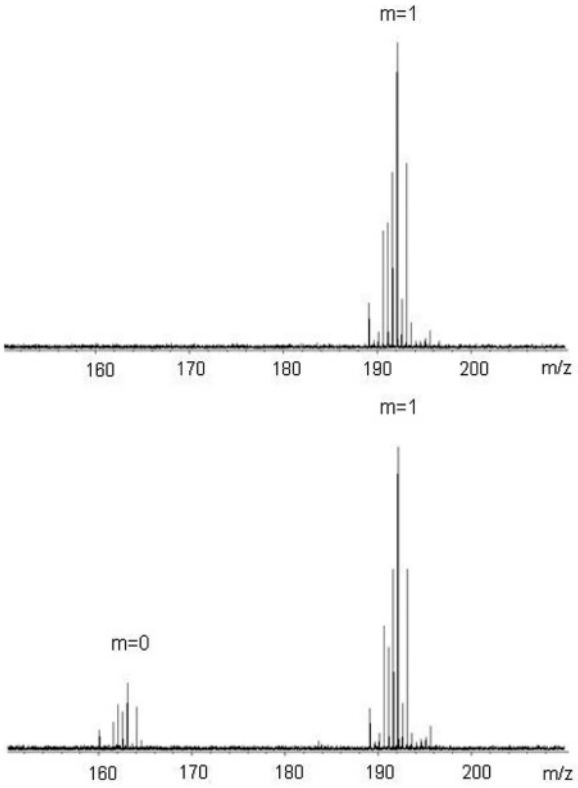

Figure 2. FTICR mass spectra of $Ru(NH_3)_2(bipy)_2^{2+}(acetone)_m$ (m = 0, 1) at 0-s (top) and 2-s (bottom) trapping time in the ICR cell.

The RRKM-based results from CWRU and from Marshall (both using kinetic modeling with a moderately loose transition state) are in generally acceptable agreement, and represent our best estimate of the kinetic parameters appropriate to the observed BIRD dissociations. Note that the similarity of the dissociation processes and the modeling choices between Paper I and the present work means that any major errors arising from inappropriate kinetic modeling are likely to be the same in both sets of results. Thus, comparisons between them should have a high degree of confidence, even if the absolute solvation energies are not accurate.

Results and Discussion

The results described in Paper I[37] have shown that reasonable gas-phase desolvation energies for various solvents (acetonitrile, acetone, and methylethyl ketone) attached to tris(2,2′-bipyridine)ruthenium(II), $[Ru(bipy)_3]^{2+}$, could be obtained using BIRD methodology. The intent of the research reported here was to study the effect of different inner-sphere ligands, namely ammine and methylpyrazine groups, on the unimolecular dissociation reactions of partially solvated ruthenium complex ions.

The first complex ion studied was $[Ru(NH_3)_2(bipy)_2]^{2+}$ solvated with different numbers of acetone molecules. The ZINDO optimized structure of the $Ru(NH_3)_2(bipy)_2^{2+}$ isomer used in subsequent calculations is shown in Figure 1a.

Upon extended trapping in the ICR cell, solvated $Ru(NH_3)_2(bipy)_2^{2+}$ undergoes dissociation by losing solvent molecules in a stepwise fashion. Figure 2 shows the mass spectrum of isolated $Ru(NH_3)_2(bipy)_2^{2+}(acetone)_1$ at two different reaction delay times. It is apparent from the mass spectra that dissociation occurs with increasing ion-trapping time, which is considered to be induced predominantly by absorption of blackbody radiation.

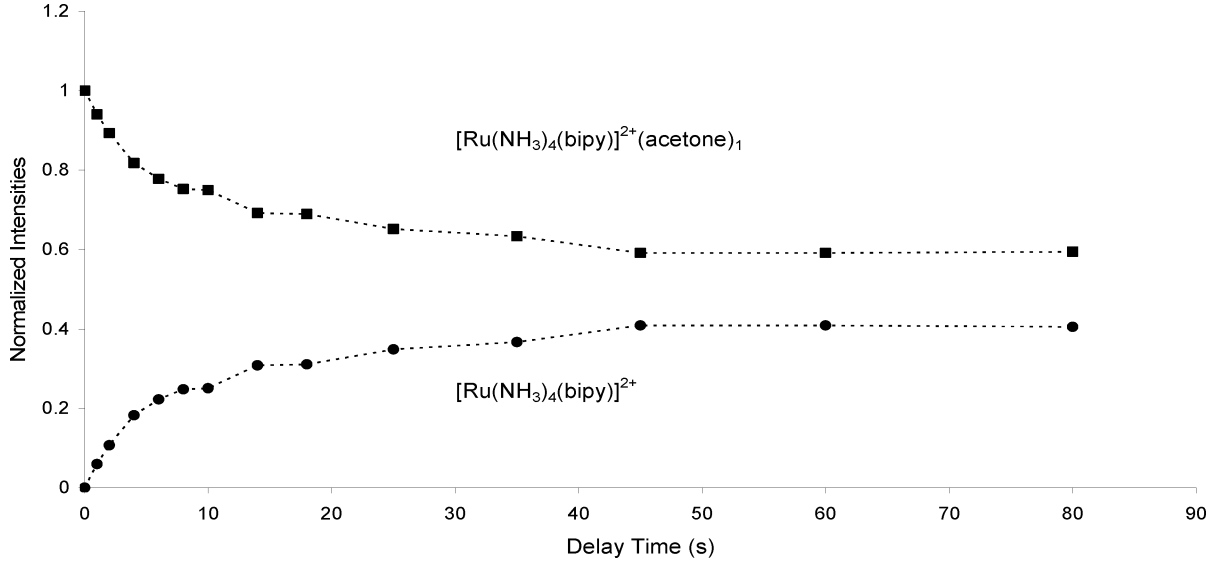

Figure 3. Appearance/disappearance curves for the loss of solvent molecule from $Ru(NH_3)_4(bipy)^{2+}(acetone)_1$ at 294 K.

The rate constant for the dissociation of $Ru(NH_3)_2(bipy)_2^{2+}$-$(acetone)_1$ is (0.16 ± 0.01) s^{-1} at 302 K, a value around 1/3 that of the dissociation rate observed for $Ru(bipy)_3^{2+}(acetone)_1$.[37] This lower dissociation rate probably reflects stronger binding of the acetone solvent molecule to the complex in the present case, as is indicated more definitively by the kinetic modeling described below.

The next complex ion studied in the series of mixed ligand ruthenium species was $Ru(NH_3)_4(bipy)^{2+}$ (Figure 1b) solvated by one or two acetone molecules. With the substitution of ammine groups in place of the bipyridine rings, we observed qualitatively a more efficient solvation of the molecular ion with acetone, as the "bare" molecular ion peak quickly disappears from the mass spectrum after introduction of the solvent-carrier gas into the ESI source housing. Moreover, a further indication of stronger solvation than for the complexes of Paper I[37] was the observation that the loss of acetone solvent molecules from the ruthenium complex ion is slower than with the solvated clusters previously studied, as indicated by the lower dissociation rate constant values measured for these desolvation reactions.

In the case of $Ru(NH_3)_4(bipy)^{2+}(acetone)_1$, the dissociation of the solvent molecule does not go to completion at the lowest temperatures used in this work. Results at 294 K illustrate this behavior, as displayed in Figure 3. After introduction of the $Ru(NH_3)_4(bipy)^{2+}(acetone)_1$ ion, dissociation occurs at a measurable rate in the 0 to 20 s time range, but at longer reaction delay times the ratio of dissociated to undissociated peak heights becomes constant, and complete dissociation to form the desolvated parent ion is not seen even at the longest delay times. Only for temperatures at or above 320 K was full dissociation of $Ru(NH_3)_4(bipy)^{2+}(acetone)_1$ observed at long delay times. The complexity of these dissociation kinetics and the limited temperature range over which dissociation could be observed to proceed to completion precluded determination of meaningful zero-pressure activation energies for the dissociation of $Ru(NH_3)_4(bipy)^{2+}(acetone)_1$ using the current experimental setup.

It is postulated that the partial dissociation of $Ru(NH_3)_4$-$(bipy)^{2+}(acetone)_1$ reflects the initial presence of two solvated isomers, one with the acetone bound to the bipy ligand, and the other with it bound to one or more of the ammine ligands. Calculations at the ZINDO level of theory were performed on the two isomers of the solvated complex ions to provide an estimate of the solvent/complex dissociation energies. The acetone/bipyridine bond energy value (32.3 kcal/mol) was 34.6 kcal/mol lower than the acetone/ammine bond energy value (66.9 kcal/mol). While absolute solvation energies by this semiempirical method would not be expected to be reliable, the difference in energies should, for qualitative purposes, be a reasonable estimate of which bonding interaction is stronger.

Although the incomplete dissociation of $Ru(NH_3)_4(bipy)^{2+}$-$(acetone)_1$ could not be analyzed to obtain thermochemical results, it was possible to determine acetone desolvation information for this complex through observations of it solvated with two acetone molecules. Figure 4 illustrates the loss of one acetone from $Ru(NH_3)_4(bipy)^{2+}(acetone)_2$ versus ion trapping time at several temperatures within the range 300 to 365 K.

Finally, the dissociation kinetics and energetics of partially solvated $Ru(NH_3)_5MePyz^{3+}$ ions (Figure 1c) were also studied. Stepwise rate constants for the desolvation reaction of $Ru(NH_3)_5$-$MePyz^{3+}(acetone)_6$ have been measured for the following reactions:

$$[Ru(NH_3)_5MePyz]^{3+}(acetone)_6 \rightarrow [Ru(NH_3)_5MePyz]^{3+}(acetone)_5 + acetone \quad (1)$$

$$[Ru(NH_3)_5MePyz]^{3+}(acetone)_5 \rightarrow [Ru(NH_3)_5MePyz]^{3+}(acetone)_4 + acetone \quad (2)$$

$$[Ru(NH_3)_5MePyz]^{3+}(acetone)_4 \rightarrow [Ru(NH_3)_5MePyz]^{3+}(acetone)_3 + acetone \quad (3)$$

To measure the rate constants with minimal contributions from side reactions with reactive species in the ICR cell, ejection of interfering ions was performed, giving isolation of the ion of interest in the FTICR cell. In the present case, the ion $Ru(NH_3)_5MePyz^{3+}(acetone)_6$ was isolated, and its subsequent sequential dissociations according to reactions 1−3 were followed.

After isolation, mass spectra were taken over an extended range of delay times to yield ion abundance data as illustrated in Figure 5. Rate constants were determined by fitting the ion peak heights as a function of trapping time using a kinetics program, Kinetica98 Beta,[48] written by one of us. Figure 5 shows

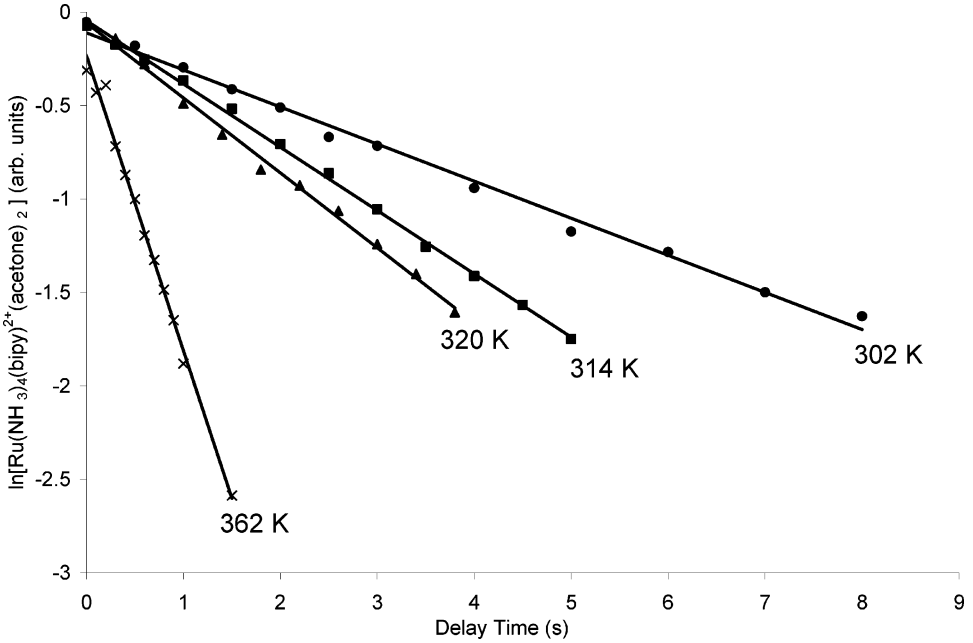

Figure 4. Semilog plots of $[Ru(NH_3)_4(bipy)^{2+}(acetone)_2]$ versus ion trapping time at several temperatures. $k(302\ K) = 0.20 \pm 0.01\ s^{-1}$, $k(314\ K) = 0.34 \pm 0.04\ s^{-1}$, $k(320\ K) = 0.40 \pm 0.02\ s^{-1}$, $k(362\ K) = 1.58 \pm 0.10\ s^{-1}$.

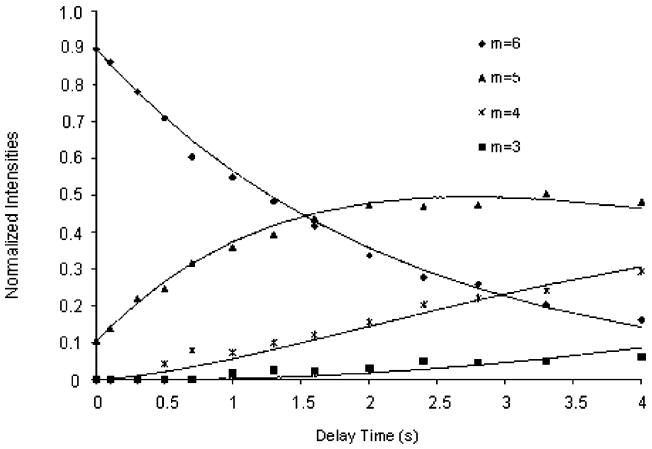

Figure 5. Appearance/disappearance curves for the dissociation of $Ru(NH_3)_5MePyz^{3+}(acetone)_m$. The solid lines through the points are calculated fits obtained by a kinetics computational program ($k_{6-5} = 0.46s^{-1}$, $k_{5-4} = 0.24s^{-1}$, $k_{4-3} = 0.15s^{-1}$).

appearance/disappearance curves associated with the dissociation of $Ru(NH_3)_5MePyz^{3+}(acetone)_6$, along with the fits from the Kinetica98 Beta analysis. The results presented in Figure 5 demonstrate the excellent fits obtained by assuming a stepwise dissociation mechanism and thus confirm such a mechanism for the dissociation reactions studied here.

H/D Isotope Effects. In a further effort to confirm BIRD as the mechanism responsible for the desolvation reactions of $Ru(NH_3)_5MePyz^{3+}(acetone)_6$, deuterium exchange studies were performed. Tonner et al.[17] showed that the BIRD mechanism leads to an expectation of a significant isotope effect on the dissociation rate when deuterium is substituted for hydrogen in the dissociating complex. Their study showed an enhancement of the BIRD rates for several types of weakly bound cluster ions. Similarly, deuterium substitution would be expected to perturb the BIRD rates in the systems studied here, and $Ru(NH_3)_5MePyz^{3+}(acetone)_m$ ions were chosen as specific cases to test this expectation. Indeed, enhanced dissociation was observed for the corresponding deuterated counterparts of several $Ru(NH_3)_5MePyz^{3+}(acetone)_m$ ions, namely the $Ru(ND_3)_5MePyz^{3+}(acetone)_m$ ions. Figure 6 shows the kinetic plots for loss of a solvent molecule from $Ru(NH_3)_5MePyz^{3+}(acetone)_8$ and $Ru(ND_3)_5MePyz^{3+}(acetone)_8$ at 294 K. With the substitution of the ammine group hydrogens by deuterium, the increase in the slope of $\ln[Ru(ND_3)_5MePyz^{3+}(acetone)_8]$ versus time is indicative of an enhanced dissociation rate.

Table 1 gives the dissociation rate enhancement percentage observed upon deuterium substitution for $Ru(NH_3)_5MePyz^{3+}(acetone)_8$ as well as three other ions in this series. As expected, the rate constants are different for the deuterated as opposed to the undeuterated species, giving further evidence of the BIRD mechanism. Other than the consistently larger dissociation rates for deuterated versus hydrogenated species, there is no apparent pattern in the dissociation enhancements observed.

Kinetic Analysis and Master Equation Modeling. It is well-known that activation energies derived from simple Arrhenius-type plots in BIRD experiments like these are typically lower than the true dissociation energies by large amounts. Further analysis of the results is essential if meaningful information about the solvation thermochemistry is to be extracted from the data. This can be done conveniently and accurately by master-equation (ME) modeling.

To perform accurate ME modeling, reasonable values of the vibrational frequencies and IR band intensities of the parent ion must be assigned. Since many of these values are not experimentally known, density functional and semiempirical calculations have been performed. Calculation of vibrational frequencies using a DFT method is possible for small complexes and may be possible for complexes solvated with one or two acetone molecules. Table 2 shows selected vibrational frequencies for $Ru(NH_3)_6^{2+}$ from ZINDO and DFT calculations as well as experimentally available values.[49,50]

The results suggest that infrared frequencies and intensities calculated using the DFT method are accurate enough for ME simulations; however, for solvated complexes involving more than two acetone molecules, DFT was not feasible and ZINDO computational methods were used. The semiempirical method yields vibrational frequencies of the C−H and N−H stretching modes that are systematically quite high. However, it is possible to correct these frequency values with an adjustment factor

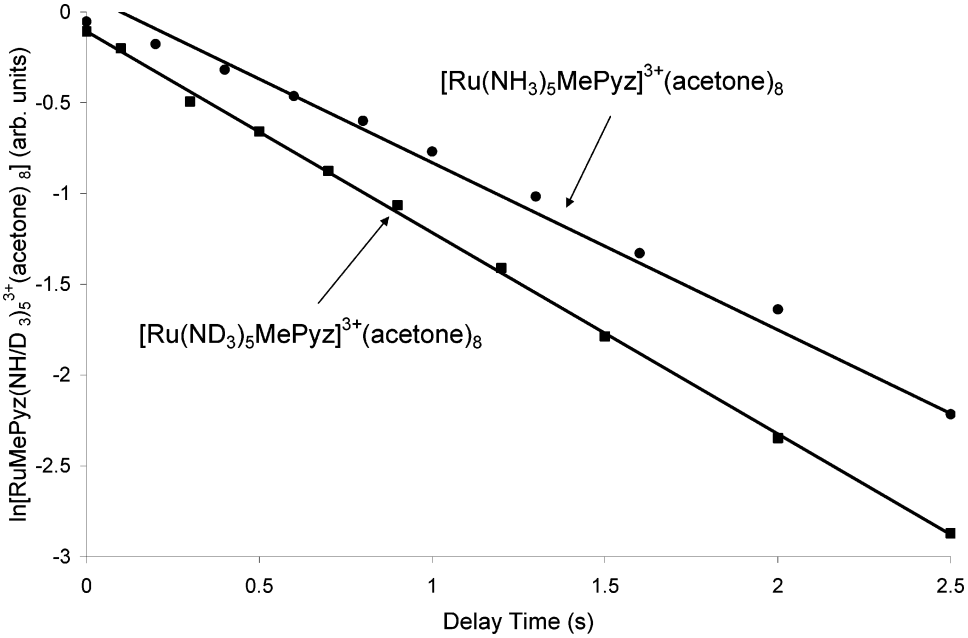

Figure 6. Semilog plots of $[Ru(NH_3)_5MePyz^{3+}(acetone)_8]$(●) and its deuterated counterpart (■) versus ion trapping time. The dissociation rate in this case has been enhanced by 17% upon deuterium substitution.

TABLE 1: Dissociation Rate Constants for $Ru(NH_3)_5MePyz^{3+}(acetone)_m$ and Their Deuterated Counterparts

dissociation pathway $Ru(NL_3)_5MePyz^{3+}(acetone)_m \rightarrow Ru(NL_3)_5MePyz^{3+}(acetone)_{m-1}$	k_{uni} (s^{-1}) L = H	k_{uni} (s^{-1}) L = D	% dissociation rate enhancement
(1) m=6	0.46 ± 0.05*	0.57 ± 0.06*	19 ± 2%
(2) m=7	0.74 ± 0.02	1.10 ± 0.16	33 ± 5%
(3) m=8	0.92 ± 0.06	1.11 ± 0.03	17 ± 1%
(4) m=12	2.30 ± 0.24	3.58 ± 0.39	36 ± 5%

*No statistical error estimates could be obtained due to the nature of the data analysis. A 10% error has been conservatively assigned.

TABLE 2: Comparison of Selected Experimental Vibrational Modes for $Ru(NH_3)_6^{2+}$ to Those Obtained by ab initio and Semiempirical Methods

vibrational mode	experimental (cm^{-1})[a]	B3LYP/LANL2DZ[b] (Gaussian 98, cm^{-1})	ZINDO[c] (HyperChem, cm^{-1})
υ_s (NH_3)	3210	3212	3260
δ_s (H-N-H)	1220	1275	1212
ρ (NH_3)	763	703	680
υ (Ru-N)	409	329	620
δ (N-Ru-N)	248	197	275

[a] Taken from Schmidt and Muller.[49, 50] [b] Scaled by 0.94. [c] Scaled using equation given in Paper I.

(given in Paper I[37]). The average deviation of the adjusted ZINDO frequencies from experiment has been found generally to be less than 100 cm^{-1}. Moreover, the high-frequency vibrational modes that are subject to this adjustment make at most a small contribution to the overall emission and absorption rates of IR radiation in these systems. Previous results comparing master equation dissociation energies calculated with DFT vs ZINDO vibrational frequencies have shown that the two computational approaches are almost identical in outcome.[37] Therefore, we have confidence that master equation modeling using these frequencies and intensities is no less reliable than that using directly calculated DFT values.

A different check on the quality of the DFT and ZINDO calculations can be made by comparing calculated Ru−N bond distances with those obtained by X-ray crystallography (as found in the Cambridge Structural Database)[51] for similar compounds. The average difference between calculated and experimental bond distances was less than 0.05 Å for 14 different Ru−N bond distances so compared, giving further confidence in the theoretically calculated parameters for these Ru complexes.

$Ru(NH_3)_2(bipy)_2^{2+}(acetone)_1$. The dissociation rates of $Ru(NH_3)_2(bipy)_2^{2+}(acetone)_1$ at several different temperatures (Figure 7) can provide the necessary thermodynamic information to describe the acetone interaction with the $Ru(NH_3)_2(bipy)_2^{2+}$ complex ion.

The dissociation rate constant values from Figure 7 were employed in Arrhenius-type analysis, shown in Figure 8, to extract a zero-pressure activation energy for the dissociation of $Ru(NH_3)_2(bipy)_2^{2+}(acetone)_1$. The activation energy obtained from the Arrhenius plot is 7.3 ± 0.5 kcal/mol.

The bond energies determined from the master equation modeling are given in Table 3. As a comparison, a dissociation energy of 15.5 kcal/mol[37] was found for the loss of acetone from $[Ru(bipy)_3]^{2+}(acetone)_1$, suggesting that the interaction between the solvent molecule and the ruthenium complex ion is strengthened (by about 4 kcal/mol) when bipyridine rings are replaced with ammine groups.

$Ru(NH_3)_4(bipy)^{2+}(acetone)_2$. As is seen in Figure 4, linear fits of experimental data points ($ln([Ru(NH_3)_4(bipy)^{2+}(acetone)_2])$ vs ion trapping time) are quite good ($R^2 > 0.98$). The rates obtained from the slopes of these plots were used to generate an Arrhenius plot (Figure 9). For the dissociation of $Ru(NH_3)_4(bipy)^{2+}(acetone)_2$ to form $Ru(NH_3)_4(bipy)^{2+}(acetone)_1$, the zero-pressure activation energy was calculated to be 7.4 ± 0.4 kcal/mol. The master-equation modeled dissociation energy was near (or slightly above) 19 kcal/mol. These results are similar to those obtained for the dissociation of $Ru(NH_3)_2(bipy)_2^{2+}(acetone)_1$

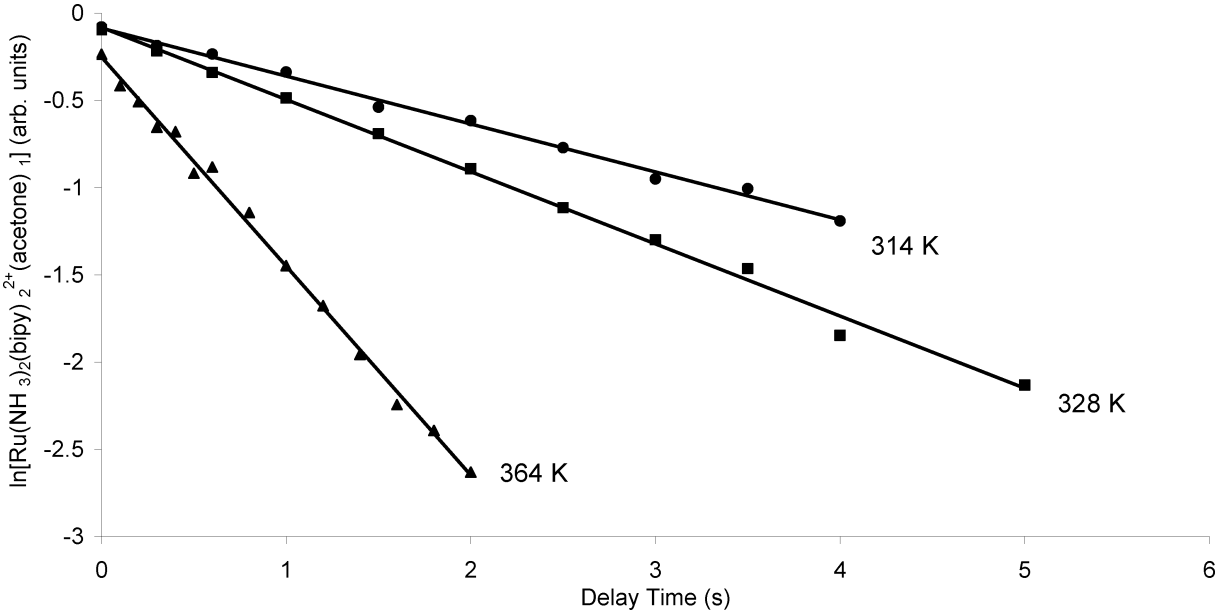

Figure 7. Semilog plots of $[Ru(NH_3)_2(bipy)_2^{2+}(acetone)_1]$ versus ion trapping time at several temperatures. $k(314\ K) = 0.27 \pm 0.02\ s^{-1}$, $k(328\ K) = 0.40 \pm 0.02\ s^{-1}$, $k(364\ K) = 1.20 \pm 0.05\ s^{-1}$.

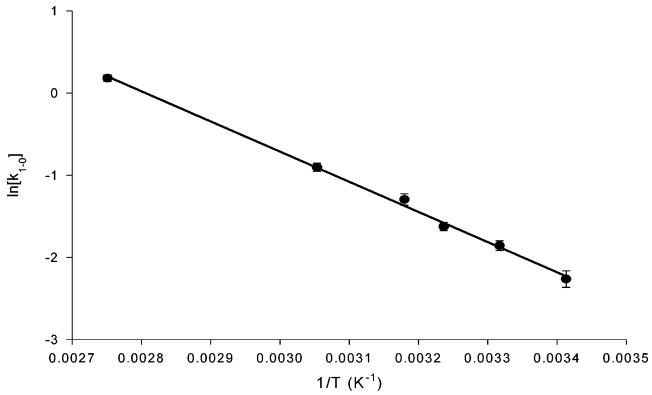

Figure 8. Arrhenius plot [ln(k) versus $1/T$] for the dissociation of $Ru(NH_3)_2(bipy)_2^{2+}(acetone)_1$.

TABLE 3: Zero-pressure Activation Energies and E_o Values Obtained from Master Equation (ME) Modeling for the Dissociation of Various Mixed Ligand Solvated Ru(II) Complex Ions

solvated complex ion	E_a (kcal/mol)	E_o[a] (kcal/mol)	E_o[b] (kcal/mol)
$Ru(NH_3)_2(bipy)_2^{2+}(acetone)_1$	7.3 ± 0.5	19.4 ± 1 (20.5)	18.9 ± 1.0
$Ru(NH_3)_4(bipy)^{2+}(acetone)_2$	7.4 ± 0.4	19.4 ± 1 (20.8)	18.8 ± 1.1
$Ru(NH_3)_5(MePyz)^{3+}(acetone)_6$	7.7 ± 1.5	18.8 ± 1	19.2 ± 0.8

[a] CWRU ME modeling, numbers in parentheses represent E_o values obtained with PST-characterized transition states. [b] Marshall University ME modeling.

which suggests a similar conformation for the second acetone around the ruthenium complex ion.

$Ru(NH_3)_5MePyz^{3+}(acetone)_6$. Desolvation energetics of $Ru(NH_3)_5MePyz^{3+}(acetone)_6$ were investigated by studying the dissociation of this solvated complex ion at different temperatures. Figure 10 displays $\ln[Ru(NH_3)_5MePyz^{3+}(acetone)_6]$ versus time data for the loss of solvent molecule from $Ru(NH_3)_5MePyz^{3+}(acetone)_6$ at several temperatures. From Arrhenius analysis, a zero-pressure activation energy value of 7.7 ± 1.5 kcal/mol was obtained. The master-equation modeled dissociation energy (Table 3) is near 19 kcal/mol. These results are again similar to the acetone/complex activation energy determined for the other ammine-containing ruthenium complex ions.

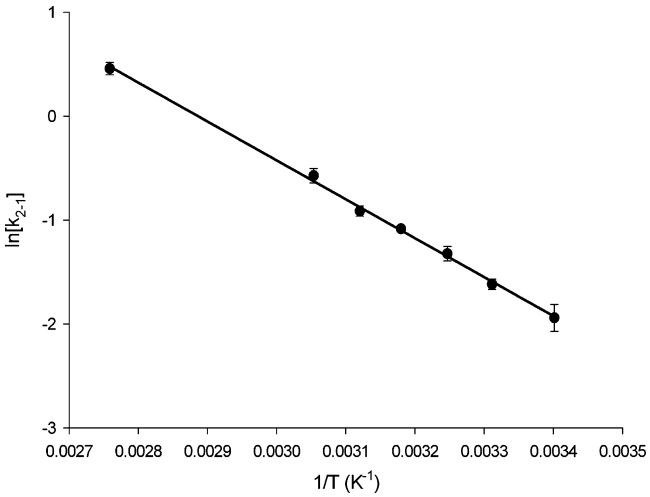

Figure 9. Arrhenius plot [ln(k) versus $1/T$] for the loss of one acetone molecule from $Ru(NH_3)_4(bipy)^{2+}(acetone)_2$.

Since increasing numbers of solvent molecules around a core ion tend to decrease the strength of binding of an additional molecule of solvent, it is interesting to observe that the solvent dissociation energy obtained for this ion is comparable to that of other ruthenium complex ions with lower extents of solvation (previously studied cases in Paper I,[37] as well as the other ions in the present study). Two compensating effects can be considered to bring this about. On one hand, the more extensive solvation shell of $Ru(NH_3)_5MePyz^{3+}(acetone)_6$, in comparison with other cases having only one or two solvent molecules, is likely to lead to lower desolvation energy. On the other hand, this ionic core with a $+3$ charge is expected to give stronger electrostatic binding of solvent molecules than the $+2$ charge on the other ions in this comparison, leading to a tendency toward higher desolvation energy for this ion.

The mass spectra obtained with $Ru(NH_3)_5MePyz^{3+}$ were dominated by highly acetone-solvated ions, especially $Ru(NH_3)_5MePyz^{3+}(acetone)_6$. This made it impossible to carry out meaningful kinetic studies of this complex ion with low degrees of solvation. Even under CID conditions, which should tend to strip off solvent molecules by imparting higher internal energy

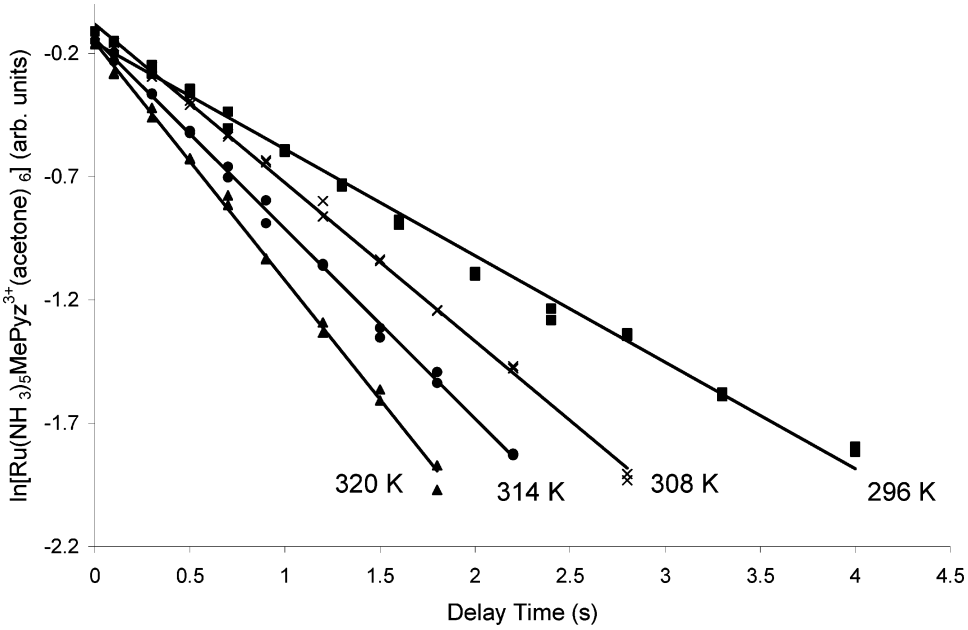

Figure 10. Semilog plots of $[Ru(NH_3)_5MePyz^{3+}(acetone)_6]$ versus ion trapping time at several temperatures. $k(296\ K) = 0.43 \pm 0.02\ s^{-1}$, $k(308\ K) = 0.77 \pm 0.02\ s^{-1}$, $k(314\ K) = 0.96 \pm 0.03\ s^{-1}$, $k(320\ K) = 1.26 \pm 0.06\ s^{-1}$.

to the precursor species, no ion was observable with an *m*/*z* value lower than that of $Ru(NH_3)_5MePyz^{3+}(acetone)_3$. This supports the supposition that the $Ru(NH_3)_5MePyz^{3+}$ core ion binds the first one or two acetone solvent molecules very tightly.

Solvation Energy Effects. Solvent binding energies previously calculated[37] for acetone and acetonitrile bound to the bipyridine ring of $Ru(NH_3)_4(bipy)^{2+}$ at the B3LYP/LANL2DZ level of theory were 15.2 and 17.0 kcal/mol for the acetonitrile and acetone interaction, respectively. These results are consistent with E_0 values obtained from experiment via ME modeling. DFT detachment energies for acetone bound to $Ru(NH_3)_4(bipy)^{2+}$-$(acetone)_2$ and $Ru(NH_3)_2(bipy)_2{}^{2+}(acetone)_1$ were calculated in the present work to be 26.9 and 24.5 kcal/mol, respectively. In this case, the agreement between theory and values obtained combining experimental results with master equation modeling (Table 3) is not as good, but it should be noted that the low quality of the basis set (LANL2DZ) used for DFT calculation of binding energies adds additional uncertainty to these energy values. Accordingly, the experimental results (with ME modeling) are considered to give a better estimate than the low-level calculations for the typical energy of acetone attachment in the outer sphere of these Ru(II) complexes, which we assign as 19 $\pm$ 1 kcal/mol.

These results are slightly higher than the previously reported E_0 value (15.5 kcal/ mol) for the solvent-complex dissociation pathway of tris(2,2′-bipyridine)ruthenium(II) solvated with acetone. They are also higher than the average value of 17.5 kcal/mol for tris(2,2′-bipyridine)ruthenium(II) solvated with between one and four molecules of methyl ethyl ketone. These differences are consistent with the idea that upon introduction of ammine groups in place of bipyridine ligands, several interactions of the acetone molecule with the complex may become more favorable: (a) a stronger interaction can occur due to hydrogen bonding to the ammine ligand; (b) a geometrical effect can occur due to the smaller radius of the ammine ligand (which allows closer approach of the solvent molecule to the charged metal, effectively increasing the ion−dipole and ion-induced-dipole electrostatic interactions); and (c) with more ammine groups coordinatively bound to the ruthenium ion in place of a bulky ligand such as bipyridine, the carbonyl oxygen from the acetone has a greater probability to be hydrogen-bonded to the ammine groups rather than to be weakly attracted to the bipyridine ring. Thus, the stronger binding of acetone assigned to the present cases, compared with the complex having only bipyridyl ligands, is in line with expectations.

As discussed more fully in Paper I,[37] solvation energies in the range 15−20 kcal/mol are quite reasonable for these Ru(II) complexes. Peschke et al.,[52] in high-pressure gas-phase equilibrium measurements, determined ΔH values for solvation that decreased from 26 to 11 kcal/mol for the 6th through 14th water molecules surrounding dipositive alkaline earth ions. For these solvated ions, six water molecules form the first solvation shell, with the subsequent solvent molecules added to a second (or higher) shell. Values for the 7th and 8th water molecules for the various alkaline earth ions were found to be in the range 15−18 kcal/mol. Rodriguez-Cruz et al.[28] used the BIRD technique to study similar systems, and obtained E_0 values that decreased from 26 to 15 kcal/mol for the 5th through 7th solvating water molecule. The E_0 values for the 7th water molecule ranged from 15 to 17 kcal/mol depending on the alkaline earth ion. The bipy and ammine ligands in the Ru(II) complexes studied in this work act as a first solvation shell around the central ion. Thus, the 1st through 6th solvents added would be similar to the 7th and subsequent water molecules added to the alkaline earth ions in the Peschke et al.[52] and Rodriguez-Cruz et al[28] studies.

Conclusions

For the solvated Ru(II) complex ions studied here, metastable dissociation can be ruled out as the desolvation mechanism, considering that the time scale of the desolvation reactions is on the order of milliseconds to several hundred seconds. Furthermore, the low pressures used in this study appear to rule out collisional activation to form "hot" ions, but rather suggest a thermally induced dissociation reaction mechanism. Hydrogen/deuterium isotope effect experiments, in which ammine group hydrogens were replaced with deuterium prior to gas-phase formation of the partially solvated complex ions, have shown that dissociation rates can be enhanced by changes in the vibrational frequencies and infrared intensities induced by

"heavy" atom substitution. These results further support the postulated BIRD mechanism.

Detailed analysis of the temperature dependence of the solvent/complex dissociation rates indicates that the activation energy obtained from the Arrhenius equation is substantially lower than the true dissociation energy, E_0. The values of E_0 obtained by master equation modeling are in the range 19 ± 1 kcal/mol. This result is almost 4 kcal/mol higher than that previously reported for $[Ru(bipy)_3]^{2+}(acetone)_1$ and is also about 2 kcal/mol higher than for several $[Ru(bipy)_3]^{2+}(methyl\ ethyl\ ketone)_n$, $n = 1-4$, complexes. This presumably reflects a stronger interaction of the solvent with the Ru(II) complex ion due to hydrogen bonding, combined with increased electrostatic interactions resulting from geometrical changes, when the complex contains some NH_3 ligands. The Ru(III) complex $Ru(NH_3)_5MePyz^{3+}(acetone)_6$ gave a desolvation energy very similar to the value found for the Ru(II) complexes, a result that was attributed to the compensating effects of higher electric charge of the ionic core versus a more extensive and crowded shell of solvent around the core.

Acknowledgment. This work was supported in part by the National Science Foundation (Grant No. CHE 97-27571). R.C.D. acknowledges the support of the donors of the Petroleum Research Fund, administered by the American Chemical Society. We thank Dr. K. Abboud for providing access to the Cambridge Structural Database and for assisting with the search to obtain Ru−N bond distances from it.

References and Notes

(1) Gerardi, R. D.; Barnett, N. W.; Lewis, S. W. *Anal. Chim. Acta* **1999**, *378*, 1.
(2) Kalyanasundaram, K. *Coord. Chem. Rev.* **1982**, *46*, 159.
(3) Meyer, T. J. *Prog. Inorg. Chem.* **1983**, *30*, 389.
(4) Juris, A.; Balzani, V.; Barigelletti, F.; Campagna, S.; Belser, P.; Von Zelewsky, A. *Coord. Chem. Rev.* **1988**, *84*, 85.
(5) Thölmann, D.; Tonner, D. S.; McMahon, T. B. *J. Phys. Chem.* **1994**, *98*, 2002.
(6) Dunbar, R. C.; McMahon, T. B. *Science* **1998**, *279*, 194.
(7) Dunbar, R. C. *Mass Spectrom. Rev.* **2004**, *23*, 127.
(8) Price, W. D.; Schnier, P. D.; Williams, E. R. *Anal. Chem.* **1996**, *68*, 859.
(9) Gross, D. S.; Williams, E. R. *Int. J. Mass Spectrom. Ion Processes* **1996**, *158*, 305.
(10) Sena, M.; Riveros, J. M. *J. Phys. Chem. A* **1997**, *101*, 4384.
(11) Aaserud, D. J.; Guan, Z. Q.; Little, D. P.; McLafferty, F. W. *Int. J. Mass Spectrom.* **1997**, *167*, 705.
(12) Penn, S. G.; He, F.; Lebrilla, C. B. *J. Phys. Chem. B* **1998**, *102*, 9119.
(13) Chen, O. N.; Groh, S.; Liechty, A.; Ridge, D. P. *J. Am. Chem. Soc.* **1999**, *121*, 11910.
(14) Strittmatter, E. F.; Wong, R. L.; Williams, E. R. *J. Phys. Chem. A* **2000**, *104*, 10271.
(15) Price, W. D.; Schnier, P. D.; Williams, E. R. *J. Phys. Chem. B* **1997**, *101*, 664.
(16) Lin, C. Y.; Dunbar, R. C.; Haynes, C. L.; Armentrout, P. B.; Tonner, D. S.; McMahon, T. B. *J. Phys. Chem.* **1996**, *100*, 19659.
(17) Tonner, D. S.; Tholmann, D.; McMahon, T. B. *Chem. Phys. Lett.* **1995**, *233*, 324.
(18) Dunbar, R. C. *J. Phys. Chem.* **1994**, *98*, 8705.
(19) Dunbar, R. C.; McMahon, T. B.; Tholmann, D.; Tonner, D. S.; Salahub, D. R.; Wei, D. Q. *J. Am. Chem. Soc.* **1995**, *117*, 12819.
(20) Lin, C. Y.; Dunbar, R. C. *J. Phys. Chem.* **1996**, *100*, 655.
(21) Jockusch, R. A.; Williams, E. R. *J. Phys. Chem. A* **1998**, *102*, 4543.
(22) Strittmatter, E. F.; Schnier, P. D.; Klassen, J. S.; Williams, E. R. *J. Am. Soc. Mass Spectrom.* **1999**, *10*, 1095.
(23) Schnier, P. D.; Price, W. D.; Jockusch, R. A.; Williams, E. R. *J. Am. Chem. Soc.* **1996**, *118*, 7178.
(24) Price, W. D.; Schnier, P. D.; Jockusch, R. A.; Strittmatter, E. F.; Williams, E. R. *J. Am. Chem. Soc.* **1996**, *118*, 10640.
(25) Price, W. D.; Williams, E. R. *J. Phys. Chem. A* **1997**, *101*, 8844.
(26) Butcher, D. J.; Asano, K. G.; Goeringer, D. E.; McLuckey, S. A. *J. Phys. Chem. A* **1999**, *103*, 8664.
(27) Rodriguez-Cruz, S. E.; Jockusch, R. A.; Williams, E. R. *J. Am. Chem. Soc.* **1999**, *121*, 8898.
(28) Rodriguez-Cruz, S. E.; Jockusch, R. A.; Williams, E. R. *J. Am. Chem. Soc.* **1998**, *120*, 5842.
(29) Schnier, P. D.; Klassen, J. S.; Strittmatter, E. E.; Williams, E. R. *J. Am. Chem. Soc.* **1998**, *120*, 9605.
(30) Jockusch, R. A.; Price, W. D.; Williams, E. R. *J. Phys. Chem. A* **1999**, *103*, 9266.
(31) Jockusch, R. A.; Lemoff, A. S.; Williams, E. R. *J. Phys. Chem. A* **2001**, *105*, 10929.
(32) Paech, K.; Jockusch, R. A.; Williams, E. R. *J. Phys. Chem. A* **2002**, *106*, 9761.
(33) Felitsyn, N.; Kitova, E. N.; Klassen, J. S. *Anal. Chem.* **2001**, *73*, 4647.
(34) Kitova, E. N.; Bundle, D. R.; Klassen, J. S. *J Am. Chem. Soc.* **2002**, *124*, 5902.
(35) Jurchen, J. C.; Williams, E. R. *J. Am. Chem. Soc.* **2003**, *125*, 2817.
(36) Paech, K.; Jockusch, R. A.; Williams, E. R. *J. Phys. Chem. A* **2003**, *107*, 2596.
(37) Stevens, S. M.; Dunbar, R. C.; Price, W. D.; Sena, M.; Watson, C. H.; Nichols, L. S.; Riveros, J. M.; Richardson, D. E.; Eyler, J. R. *J. Phys. Chem. A* **2002**, *106*, 9686.
(38) Spence, T. G.; Burns, T. D.; Posey, L. A. *J. Phys. Chem. A* **1997**, *101*, 139.
(39) de Koning, L. J.; Nibbering, N. M. M.; van Orden, S. L.; Laukien, F. H. *Int. J. Mass Spectrom. Ion Processes* **1997**, *165/166*, 209.
(40) Ridley, J.; Zerner, M. *Theor. Chim. Acta* **1973**, *32*, 111.
(41) Ridley, J. E.; Zerner, M. C. *Theoretica Chimica Acta* **1976**, *42*, 223.
(42) Frisch, M. J.; Trucks, G. W.; Schlegel, H. B.; Scuseria, G. E.; Robb, M. A.; Cheeseman, J. R.; Zakrzewski, V. G.; Montgomery, J. A., Jr.; Stratmann, R. E.; Burant, J. C.; Dapprich, S.; Millam, J. M.; Daniels, A. D.; Kudin, K. N.; Strain, M. C.; Farkas, O.; Tomasi, J.; Barone, V.; Cossi, M.; Cammi, R.; Mennucci, B.; Pomelli, C.; Adamo, C.; Clifford, S.; Ochterski, J.; Petersson, G. A.; Ayala, P. Y.; Cui, Q.; Morokuma, K.; Malick, D. K.; Rabuck, A. D.; Raghavachari, K.; Foresman, J. B.; Cioslowski, J.; Ortiz, J. V.; Baboul, A. G.; Stenfanov, B. B.; Lui, G.; Liashenko, A.; Piskorz, P.; Komaromi, I.; Gomperts, R.; Martin, R. L.; Fox, D. J.; Keith, T.; Al-Laham, M. A.; Peng, C. Y.; Nanayakkara, A.; Gonzalez, C.; Challacombe, M.; Gill, P. M. W.; Johnson, B. G.; Chen, W.; Wong, M. W.; Andres, J. L.; Head-Gordon, M.; Replogle, E. S.; Pople, J. A., Gaussian 1998; Gaussian, Inc.: Pittsburgh, PA.
(43) Hay, P. J.; Wadt, W. R. *J. Chem. Phys.* **1985**, *82*, 270.
(44) Wadt, W. R.; Hay, P. J. *J. Chem. Phys.* **1985**, *82*, 284.
(45) Hay, P. J.; Wadt, W. R. *J. Chem. Phys.* **1985**, *82*, 299.
(46) Dunning, T. H., Jr.; Hay, P. J. *Modern Theor. Chem.* **1977**, *3*, 1.
(47) Dunbar, R. C. *Int. J. Mass Spectrom. Ion Processes* **1990**, *100*, 423.
(48) Richardson, D. E. *Kinetica98 Beta*; available at http://www.chem.ufl.edu/~der/der_soft.htm.
(49) Schmidt, K. H.; Muller, A. *Inorg. Chem.* **1975**, *14*, 2183.
(50) Schmidt, K. H.; Muller, A. *Coord. Chem. Rev.* **1976**, *19*, 41.
(51) Allen, F. H.; Kennard, O. *Chem. Des. Autom. News* **1993**, *8*, 31.
(52) Peschke, M.; Blades, A. T.; Kebarle, P. *J. Phys. Chem. A* **1998**, *102*, 9978.